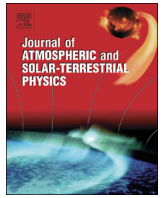




Contents lists available at ScienceDirect

Journal of Atmospheric and Solar-Terrestrial Physics

journal homepage: www.elsevier.com/locate/jastp

Catalogue of electron precipitation events as observed in the long-duration cosmic ray balloon experiment

V.S. Makhmutov, G.A. Bazilevskaya, Yu.I. Stozhkov, A.K. Svirzhetskaya, N.S. Svirzhhevsky

Lebedev Physical Institute of Russian Academy of Sciences, Leninsky Prospect, 53, 119991 Moscow, Russia

ARTICLE INFO

Article history:

Received 21 October 2015

Received in revised form

8 December 2015

Accepted 10 December 2015

Keywords:

Atmosphere

Cosmic rays

Balloon experiment

Electron precipitation

Geomagnetic disturbances

ABSTRACT

Since the International Geophysical Year (1957), the Lebedev Physical Institute performs the regular measurements of charged particle fluxes in the Earth's atmosphere (from the ground level up to 30–35 km) at several latitudes. The unique experimental data base obtained during 58 years of cosmic rays observations in the atmosphere allows to investigate temporal, spatial and energetic characteristics of galactic and solar cosmic rays as well as the role of charged particles in the atmospheric processes. Analysis of this data base also revealed a special class of numerous events caused by energetic electron precipitation recorded in the atmosphere at polar latitudes. In this paper we present Catalogue of electron precipitation events observed in the polar atmosphere during 1961–2014 and briefly outline the previous results of this data set analysis.

© 2015 Elsevier Ltd. All rights reserved.

1. Introduction

From the middle of 1957 till present the P.N. Lebedev Physical Institute of the Russian Academy of Sciences (Laboratory of Solar and Cosmic ray physics-Dolgoprudny Scientific Station) has carried out the regular balloon measurements of charged particle fluxes in the atmosphere from the ground level up to 30–35 km above the sea level. The measurements are performed at polar (northern and southern) and middle latitudes (including six latitude surveys in 1962–1987; Bazilevskaya and Svirzhetskaya (1998)). More than 85,000 measurements of cosmic ray fluxes in the atmosphere have been performed using the Geiger counters. The main goals of observations are the investigations of galactic cosmic ray modulation in the heliosphere, solar cosmic ray generation and propagation, precipitation of energetic electrons from the Earth's magnetosphere and the role of charged particles in the atmospheric processes (Charakhchyan, 1964; Bazilevskaya et al., 1991; Bazilevskaya and Svirzhetskaya, 1998; Stozhkov et al., 2001, 2009).

In this paper we focus on the magnetospheric electron precipitation into the atmosphere which is important process of the outer radiation belt depletion (e.g., Horne and Thorne, 2003). In the stratospheric experiment we deal with $E > 200$ keV electron flux. The magnetosphere reacts to the disturbed solar wind with changes of its configuration and violation of the magnetopause. The outer radiation belt populated by energetic electrons gets additional electrons both from the solar wind and the ionosphere.

The electrons are then subject of two competing processes—beta-tron or stochastic acceleration and losses via escaping back to space or into the atmosphere (Reeves et al., 2003). Currently accepted rapid loss mechanisms include magnetopause shadowing and/or outward diffusion, and precipitation to the atmosphere due to wave-particle interactions (Ukhorskiy et al., 2015).

Satellites situated in the magnetosphere observe an enhanced variability of high-energy electron fluxes not only because of real particle acceleration and loss but also because of particle spatial and energy redistribution. Therefore from the satellite observations it is not always easy to assess real electron precipitation. In the atmosphere we avoid this ambiguity. It should be noted that solar wind-magnetosphere coupling leading to electron precipitation remains still an open area for research (Blum et al., 2015; Clilverd et al., 2010; Sandanger et al., 2009).

Precipitation is a consequence of the electron scattering into the loss cone which results from the nonlinear wave-particle interaction. ULF and VLF waves are generated in the magnetosphere by interplanetary disturbances (Reeves et al., 2003). Whistler mode chorus, hiss and electromagnetic ion cyclotron waves (EMIC) can both accelerate electrons to higher energies and scatter electrons into the loss cone through resonant pitch angle interaction. In the course of the bounce and drift motions an electron passes to various regions and can be accelerated or lost. Numerous works are devoted to modeling and observation of such effects, to mention just a few: Carson et al., 2013; Clilverd et al., 2015; Kersten et al., 2011; Kubota et al., 2015; Li et al., 2013; Lorentzen et al., 2000; Meredith et al., 2002; O'Brien et al., 2003; Wang et al., 2014.

E-mail address: makhmutv@sci.lebedev.ru (V.S. Makhmutov).

Even a brief outline shows extremely complicated dynamics of magnetospheric electrons.

Study of electron precipitations is important both for fundamental science and human practice activity. Large electron fluxes affect orbital satellites causing an electrostatic discharge (ESD) anomaly. Cumulative effect of radiation damages is one of the most important factors limiting the lifetime of a spacecraft. A single energetic electron can introduce errors into memory chips and other electronic devices, known as a single-event upset (SEU). SEUs can lead to corruption of data in memory chips and to phantom commands (Horne, 2002). Additional ionization created by the electron fluxes violates the radio wave propagation in the ionosphere (Clilverd et al., 2010). Electron precipitation contributes to the production of odd nitrogen NO_x and odd hydrogen HO_x through ion-molecular reactions in the upper atmosphere. Both NO_x and HO_x can destroy odd oxygen through catalytic reactions, and hence play an important role in the ozone balance of the middle atmosphere (Clilverd et al., 2009; Turunen et al., 2009; Krivolutsky and Repnev, 2012). During the last decades enormous efforts have been undertaken for understanding and forecasting of electron precipitation. Dynamics of energetic electrons in the magnetosphere has been observed at many spacecraft missions including GOES, POES, CRRES, SAMPEX, Polar, Cluster and others. A dedicated pair of satellites – Van Allen Probes – was launched in 2012 (Spence et al., 2013). Special balloon campaigns MAXIS, MINIS, BARREL have been organized with the aim of simultaneous observation of electron fluxes in space and in the atmosphere (Millan et al., 2002, 2007; Comess et al., 2013; Sample, 2013; Woodger et al., 2015). Observations proved that the electron flux can vary by several orders of magnitude on time scales as short as a few minutes (e.g., Blake et al., 1996; Nakamura et al., 2000; Blum et al., 2015).

This paper presents the Catalogue of events of high-energy magnetospheric electron precipitation recorded by the cosmic ray group from the Lebedev Physical Institute during more than half century of cosmic ray observations in the stratosphere. Results of simulations of the energetic electron flux propagation through the Earth's atmosphere are described. These results were used for evaluation of characteristics of precipitating electron fluxes given in the Catalogue.

2. Balloon cosmic ray experiment in the Earth's atmosphere

Since the International Geophysical Year (1957), the Lebedev Physical Institute performs the regular measurements of cosmic rays in the atmosphere (Charakhch'yan, 1964; Bazilevskaya et al., 1991; Bazilevskaya and Svirzhevskaya, 1998; Stozhkov et al., 2001, 2009). Observations are taken with light balloons at several latitudes almost every day. In the frame of this program, the electron precipitation events (EPEs) are detected at polar latitudes. Information on polar stations of cosmic ray measurements in the stratosphere where these events were recorded is given in Table 1.

Balloon launching time during many year observations remained in the limits of 8–11 LT and ~13–18 LT. A typical flight lasts about 1.5 h and a balloon usually reaches altitudes where precipitation can be observed. The balloons do not remain long at high altitudes where EPEs may be observed, i.e., we usually do not record an EPE start and end as it would be possible during long-lasting balloon flights (e.g., Lazutin et al., 1982; Parks et al., 1993; Millan et al., 2002). In spite of the fact that observational time at Murmansk region and at Mirny observatory was close, almost all of EPEs were recorded at Murmansk region. This is because Mirny is located in the polar cap, mainly at the open geomagnetic field lines (Makhmutov et al., 2002).

Simultaneous observations of the EPEs at the different locations are very important from the point of view of estimation of longitudinal extension of energetic electron precipitation region. Such simultaneous balloons being at the same atmospheric altitude at any two stations during the EPE are rather rare occasion. Table 2 presents a comparative statistics of few electron precipitation events observed simultaneously at pair of stations Olenya-Norilsk and Olenya – Tixie Bay.

In spite of small statistics of events recorded at Norilsk and Tixie Bay, it is possible to conclude that (1) the events recorded at Norilsk in ~30% of cases were also recorded at Olenya, and contrary, the events observed at Olenya in ~23% cases were also recorded at Norilsk; (2) in ~50% of cases the events recorded at Tixie Bay also were observed at Olenya, but in ~20% of cases the electron precipitation events at Olenya were seen at Tixie Bay. The fact of simultaneous observations of EPEs at well separated locations means that the energetic electron precipitation region

Table 1

List of high-latitude stations of stratospheric cosmic ray monitoring (R_c – geomagnetic cutoff rigidity).

Station	Geograph. Coordinates	R_c (GV)	Start time of balloon launch (UT)	Period of measurements	Number of balloon launches	Number of EPEs recorded till 2014
Olenya, Murmansk region	68°57'N 33°03'E	0.6	5–8	07/1957–2002	~ 40,000	524
Apatity, Murmansk region	67°33'N 33°20'E	0.6	12–15	2002–present time		
Mirny, Antarctica	66°34'S 92°55'E	0.03	6–9	03/1963–present time	16,700	10
Norilsk	69°00'N 88°00'E	0.6	5–8	11/1974–06/1982	760	10
Tixie Bay	71°36'N 128°54'E	0.5	5–8	02/1978–10/1987	1190	17

Table 2

Comparative statistics of EPEs recorded at Olenya, Norilsk and Tixie Bay.

Pair of stations ($S1$ and $S2$)		Period of measurements	Number of simultaneous launches at $S2$	Number of EPEs recorded at the $S1$	Number of EPEs recorded simultaneously at $S1$ and $S2$
$S1$	$S2$				
Olenya	Norilsk	11/1974–06/1982	13	89	3
Norilsk	Olenya	11/1974–06/1982	10	11	3
Olenya	Tixie Bay	02/1978–10/1987	47	145	9
Tixie Bay	Olenya	02/1978–10/1987	16	17	9

sometimes is widely extending over a longitude $\sim 80^\circ$. Also we point out that even though the observation of same event at pair stations is not absolutely at one time, the significant fluxes of very energetic photons were recorded at both sites.

3. Selection of the electron precipitation events

The probe for measuring of cosmic rays consists of two Geiger tubes arranged as a telescope with a 7 mm (2 g cm^{-2}) thick Al filter inserted between the counters. A single counter is sensitive to electrons ($E > 200 \text{ keV}$), protons ($E > 5 \text{ MeV}$), and X-rays ($E > 20 \text{ keV}$, efficiency $\approx 1\%$), and a telescope records electrons ($E > 5 \text{ MeV}$) and protons ($E > 30 \text{ MeV}$). Efficiency of the charged particles recording is close to 100%. A radio pulse caused by a charged particle passing through a counter or a telescope and information on the residual air pressure is transmitted to the ground-level receiver (more details are in Charakhch'yan, 1964; Bazilevskaya et al., 1991; Bazilevskaya and Svirzhevskaya, 1998; Stozhkov et al., 2001, 2009).

We identified an EPE if we observe an enhancement of the count rate of a single counter by $> 30\%$, but not of a telescope. The enhancement observed at altitude more than 20 km above the sea level lasts at least 10 min. Actually, precipitating electrons are absorbed at levels of a few g cm^{-2} in the upper atmosphere. However, they generate X-rays that can penetrate rather deep into the atmosphere and may be detected by a single counter, which is sensitive to X-rays, but not by a telescope. In $\sim 75\%$ of EPEs recorded, X-rays propagate in the atmosphere down to $\sim 25 \text{ km}$, one third of them being registered at altitudes above 30 km. Thus, we mainly deal with precipitation of electrons with energies above several hundreds of keV (Makhmutov et al., 2001).

Figs. 1 and 2 give some examples of EPEs recorded in the atmosphere. Note that a telescope count rate does not increase while that of a single counter goes up. It is also seen that significant time variations in the X-ray flux may sometimes be observed against the quiet flux of charged particles detected by a telescope. In the absence of such variations, we assume that the electron flux at the atmospheric boundary is stable and the change in the X-ray flux is caused by the X-ray absorption in the atmosphere. Although the observations hint at variety of EPE types observed we do not make any selection by event type of the EPEs for this publication.

Vertical arrows (Fig. 2, right) show atmospheric depth levels (X_{max}) where count rates of the CR probe begin increase during the

events presented at left panel of Fig. 2. The values of X_{max} were determined for whole set of precipitation events. Analysis of the X_{max} distribution allows to conclude that majority of EPEs were observed at the atmospheric depths $X < 30 \text{ g cm}^{-2}$ (altitudes $H > 24 \text{ km}$), but in several events X-rays propagate down to $X > 50 \text{ g cm}^{-2}$ (altitudes $H < 20 \text{ km}$). Note that the bremsstrahlung photons with initial energy $E_{ph} = 0.3, 1.5$ and 3 MeV have attenuation lengths in air $X = 9.4, 19.4$ and 28.9 g cm^{-2} , correspondingly. Such energetic photons could be produced by hundreds keV – few MeV precipitating electrons at the top of the Earth's atmosphere.

To evaluate the photon absorption spectrum (ΔN values of the omnidirectional counter at different levels of X) for the events the background cosmic ray curve (curve 3 in Fig. 2) was subtracted from the curves 1 and 2 obtained during these EPEs. Results of such subtraction were shown in Fig. 2 (right panel). Line 1 and 2 show the best fit of the data in the form $\Delta N = N \cdot \exp(-X/X_0)$. Such approximation of the data allows to evaluate photon absorption spectra recorded in the atmosphere in the form $J_{ph(>20 \text{ keV})}(X) = A_{ph} \cdot \exp(-X/X_0)$. We determined such photon absorption spectrum for each electron precipitation event observed in the atmosphere. These parameters of the recorded photon absorption spectra, A_{ph} and X_0 , were used for evaluation of the energy spectrum of precipitating electrons at the top of the atmosphere for each event as it is described below.

4. Estimation of the precipitating electron flux and energy spectra

As mentioned before, during the EPEs a flux of secondary bremsstrahlung photons is generated by a precipitating electron flux at the top of the atmosphere. These photons can propagate down to altitudes of 15–20 km in the atmosphere and can be registered by a balloon-borne probe. The main characteristic of an electron precipitation event observed in the atmosphere is a photon absorption spectrum (Fig. 2, right panel; more details are in Makhmutov et al. (2003a, 2003b, 2003c)). In case of smooth increasing of the X-ray fluxes with altitude we can assume that the flux of precipitating electrons at the atmospheric boundary during the measurements is constant. In order to estimate the energy spectrum of the incident electrons we have simulated the electron transport in the atmosphere which includes the production of the secondary photons and their transport through the atmosphere,

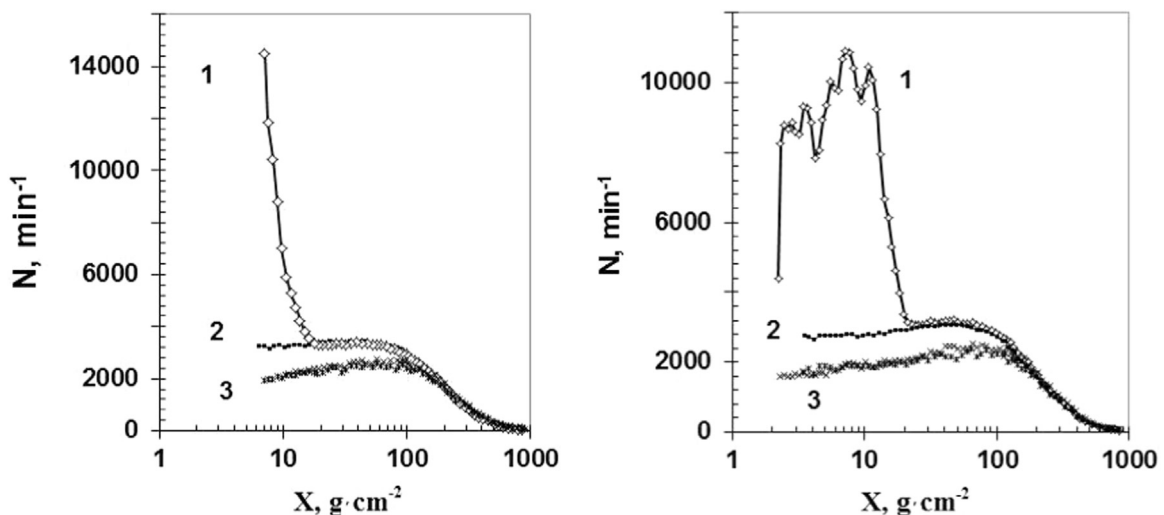


Fig. 1. Three minute averages of count rates of single counters during (1) EPEs and (2) quiet conditions, and (3) telescopes versus residual atmospheric depth (X). Count rates of telescopes are multiplied by 5. Left panel – the EPE of September 28, 1997. Right panel – EPE of October 9, 1998.

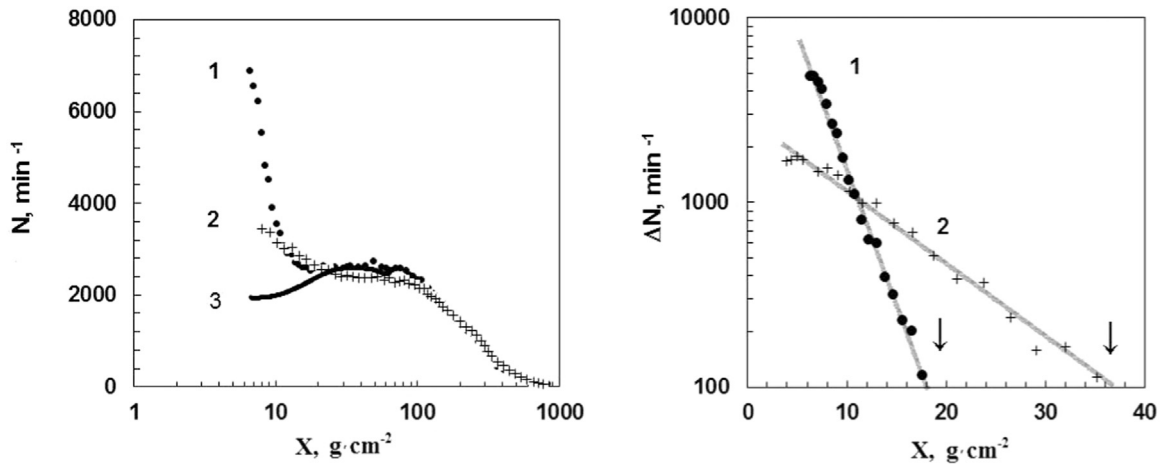


Fig. 2. *Left:* three minute averages of count rates of single counters during two EPEs (1: 29.09.1999, 08:19–09:10 UT; 2: 05.05.2000, 08:32–09:29 UT) and 3: prior to the EPEs the cosmic ray background during quiet conditions versus residual atmospheric depth. *Right:* > 20 keV photon absorption spectra (ΔN versus atmospheric depth X), where ΔN are three minutes averages of the excess of single counter rates above the background) during the EPEs 1 and 2 shown at the right panel. Line 1 and 2 show the best fit of the data in the form $\Delta N = N \cdot \exp(-X/X_0)$.

similarly to other works (e.g. Berger and Seltzer, 1972; Berger et al., 1974; Lazutin, 1979; Kalinina et al., 1988). However, our consideration was specially directed to simulation as close as possible to conditions of our balloon measurements: (a) we chose $E=20$ keV as energy threshold of photon registration by the STS-6 Geiger counter used in our CR probe; (b) the results of calculations were summarized for the range of atmospheric depth (0–60 g cm^{-2}), where the EPEs mostly were recorded in the atmosphere. In calculations we have used the Monte-Carlo ATMO-COSMICS (PLANETOCOSMICS) code based on Geant4 (Agostinelli et al., 2003; Desorgher et al., 2003; Desorgher, 2004). This code simulates the hadronic and electromagnetic interactions of energetic particles at energies $E < 100$ GeV in the Earth's atmosphere (atmospheric model MSISE90 or NRLMSISE00 or TABLE; Desorgher 2004; Picone et al., 2002). It computes the resulting flux of atmospheric shower particles at different altitudes (or atmospheric depths), the energy deposited in the atmosphere versus altitude, and the production of cosmogenic nuclides. The electromagnetic shower is simulated by taking into account the following processes: bremsstrahlung, energy loss by ionization, multiple scattering, pair production, Compton scattering, and photoelectric effect. First results of simulations of monoenergetic electron fluxes propagation in the atmosphere were presented in Makhmutov et al. (2003a). They confirm good agreement with those of Berger and Seltzer (1972).

To estimate the energy spectrum of precipitating electrons during EPEs, we made an assumption that the primary flux of precipitating electrons at the top of the atmosphere can be expressed by an exponential spectrum, $J_e(E) = A_e \cdot \exp(-E/E_0)$ (e.g. Comess et al., 2013; Lazutin, 1979, 1986; Millan et al., 2007), with characteristic energy E_0 in the range 10 keV to 1 MeV. To study the transport of primary electron flux in the atmosphere we have calculated the electron and photon energy spectra at different atmospheric depth levels. As an example in Fig. 3 we show the evolution of the energy spectrum $J_e(E) = 1 \cdot \exp(-E/300 \text{ keV})$ of incident electrons on the top of the atmosphere at selected atmospheric depth levels $X=0.05, 0.5$ and 1 g cm^{-2} (64.5, 49.9 and 45.5 km, correspondingly).

Note very significant reduction (by factor $\sim 10^{4-6}$) of primary electron fluxes already at altitude ~ 50 km ($X=0.49 \text{ g cm}^{-2}$).

Fig. 4 demonstrates the secondary photon energy spectra at several atmospheric levels. As can be seen the photon flux (e.g., at energy $E=100$ keV) at altitude 24 km decreased only by factor 15 regarding to the photon flux level at 70 km. In comparison, the

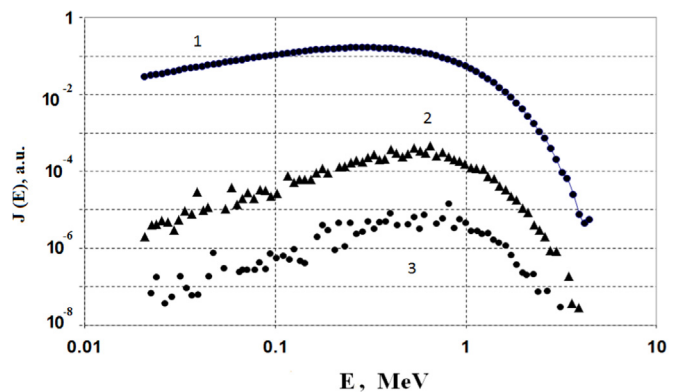


Fig. 3. Electron energy spectra at several atmospheric levels $X=0.05$ (curve 1), 0.5 (curve 2) and 1 g cm^{-2} (curve 3). Electron flux $J_e(E)$ in arbitrary units (a.u.).

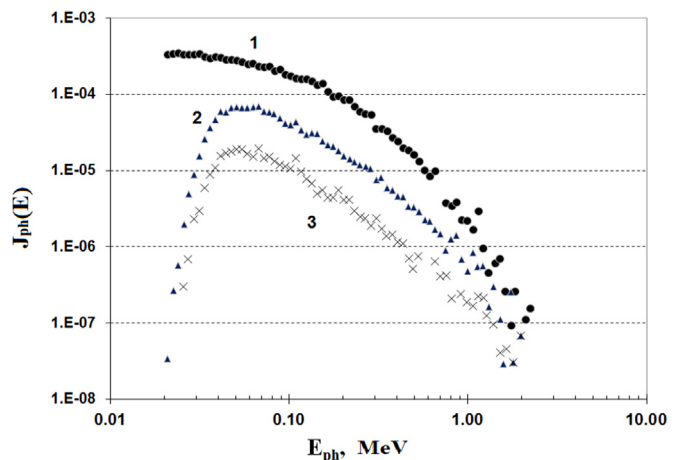


Fig. 4. Photon energy spectra at several atmospheric levels $X=0.05 \text{ g cm}^{-2}$ (altitude ~ 70 km; curve 1), $X=15 \text{ g cm}^{-2}$ (altitude=28.3 km; curve 2) and $X=30 \text{ g cm}^{-2}$ (altitude=23.9 km; curve 3). Photon flux $J_{ph}(E)$ in arbitrary units (a. u.).

secondary electron flux reduced by factor $\sim 10^7$ at those altitudes.

Finally we have computed the number of secondary photons with $E > 20$ keV at different atmospheric depths (in the range $X=0.05-50 \text{ g cm}^{-2}$) resulting from precipitation of primary electron flux with different exponential parameter E_0 . For each E_0 we have obtained a photon absorption spectrum, i.e. photon number

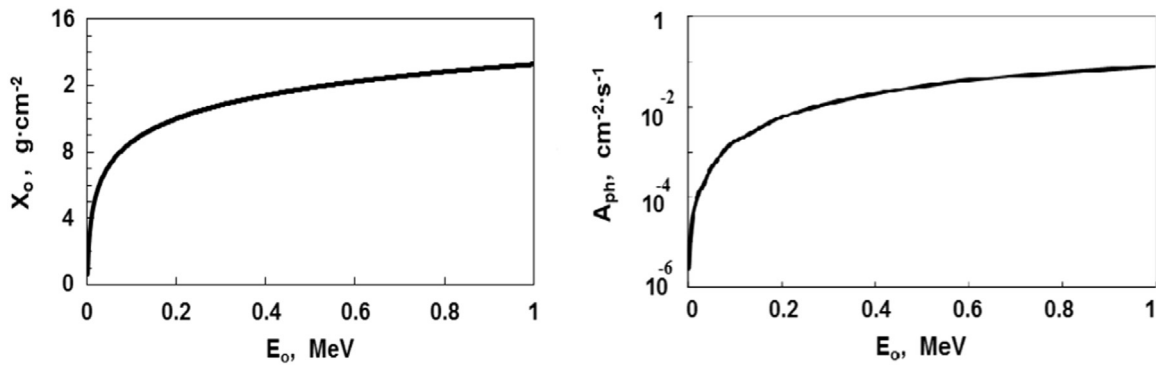


Fig. 5. Simulation results: *left panel* – the dependence of the parameter X_0 of the photon absorption spectrum in the atmosphere on the characteristic energy E_0 of the primary electron spectrum in the form of $J_e(E) = A_e \cdot \exp(-E/E_0)$; *right panel* – the correspondence between the coefficient A_{ph} of the photon spectrum and characteristic energy E_0 of the electron spectrum.

versus atmospheric depth, that we fit with an exponential law as $J_{ph}(> 20 \text{ keV})(X) = A_{ph} \cdot \exp(-X/X_0)$. Fig. 5 (left) shows the parameter X_0 of the photon absorption spectrum as a function of the characteristic energy E_0 of the primary electron spectrum. Using the results shown in Fig. 5, we can deduce the spectral parameter E_0 for a specific EPE from the parameters X_0 and J_0 of the observed absorption spectrum (Makhmutov et al., 2003a, 2006). For retrieving these parameters we have used the 3-min averaged data and fitted the experimental X-ray absorption spectrum by an exponent. Thereby we did not account for fast temporal variations of the photon flux. In the case of several separate count rate enhancements during one balloon flight we have treated only that at the highest altitudes (therefore some powerful event may be missed).

This procedure was applied to each EPE and the results are presented in the Table A1 as the Catalogue of EPEs recorded by our group in the course of the long-term charged particle fluxes monitoring in the stratosphere since 1957 (see Attachment). Some precipitations take place during intrusion into magnetosphere of solar energetic particles. Only one event was discussed in (Bazilevskaya et al., 2002). Such events are not included in this data set and will be analyzed later.

For each precipitation event in the Catalogue the following information is given:

- event number,
- date (dd mm yyyy),
- time interval of the EPE observation (Start Time, T_0 – End Time, T_e ; hh mm hh mm, UT),
- A_e – parameter of the flux of incident electrons in $\text{cm}^{-2} \text{s}^{-1} \text{keV}^{-1}$,
- E_0 – characteristic energy of electron spectra in keV,
- $J(E > 20 \text{ keV})$ – integral flux of incident $> 20 \text{ keV}$ electrons in $\text{cm}^{-2} \text{s}^{-1}$.

It should be noted that parameters of the energy spectra (A_e and E_0) as well as the value of $> 20 \text{ keV}$ electron flux ($J(E > 20 \text{ keV})$) were obtained under assumption that the incident electron flux did not change during the time interval $T_0 - T_e$. In reality the electron flux can fluctuate rapidly on the time scale of several minutes (Blake et al., 1996; Nakamura et al., 2000; Blum et al., 2015). Therefore, the parameters A_e , E_0 and $J(E > 20 \text{ keV})$ should be considered as a first approximation or an estimation.

5. Conclusion

The time series of EPEs in the stratosphere presented in the Catalogue, were investigated in a number of works (e.g.,

Bazilevskaya and Svirzhetskaya, 1998; Makhmutov et al., 2001, 2002, 2005, 2012, and references therein). The obtained results of the analysis could be briefly outlined as follow.

1. On the long-term scale, the EPE yearly rate reaches maximum at the descending phase of solar activity cycle and correlates with occurrence of corotating high-speed solar wind streams. Apparently, the CME-related transient solar wind disturbances typical for solar maximum conditions are not very effective for EPE production in the Earth's atmosphere (Makhmutov, et al., 2003a).
2. The monthly numbers of the EPEs recorded at Olenya station (Murmansk region) show the semiannual variation with two maxima. The first one is in April and the second one is rather extended covering August–October period. We believe that the first peak is in accordance with the expectation of Russel-McPherron effect. A second peak is complex and probably due to the superposition of axial, equinoctial and Russel-McPherron effects (Makhmutov et al., 2003c, 2005).
3. On the day-to-day scale, EPEs most probably occur under southward B_z , two days after SSC, one day after maximum of the IMF B_z strength. On the EPE day, maximum values of solar wind velocity, K_p , AE , and D_{st} indices are observed. EPEs most probably happen during significant increase in the relativistic electron flux at geostationary orbit (Makhmutov et al., 2003c).

Our previous findings did not consider properties of precipitating electrons. The present Catalogue will be used for study of the relations between the parameters of the electron spectra and concomitant phenomena with the aim of better understanding of the underlying physics. An area of electron precipitation research is still very wide. More information is needed about dynamics of the energy spectra, temporal variability of precipitation, relative contribution of various mechanisms in the radiation belt depletion, depending on the type of geomagnetic disturbance. Hopefully, the present Catalogue will be useful also for modeling of atmospheric effects such as additional ionization production of NO_x and HO_x during almost five cycles of solar activity.

Acknowledgement

The cosmic ray monitoring in the atmosphere is partly supported by Russian Foundation for Basic Research Grants no.14-02-00905a, 13-02-00585, 13-02-00931, 15-02-10070k, 16-02-00100 and by the Program “High Energy Physics and Neutrino Astrophysics” of the Russian Academy of Sciences. The Catalogue of EPE was compiled during implementation of the ISSI team project

Table A.1

Catalogue of Electron Precipitation Events recorded in the long-term cosmic ray experiment in the stratosphere at the polar stations Murmansk region (Olenya, Apatity), Norilsk, Mirny and Tixie Bay. The 3-min averages of data were used. For each event the following information is given: event number date (day, month, year) time interval of the EPE observation (T_0 - T_e , Start and End Time of observation, hour, minutes), A_e – parameter of the flux of incident electrons in $\text{cm}^{-2} \text{s}^{-1} \text{keV}^{-1}$, E_0 – characteristic energy of electron spectra in keV $J(E > 20 \text{ keV})$ – integral flux of incident $> 20 \text{ keV}$ electrons in $\text{cm}^{-2} \text{s}^{-1}$.

N	Date			T_0 - T_e (UT)		A_e	E_0 , keV	$J(E > 20 \text{ keV})$		
1	9	5	1961	8	15	8	27	6.52E+06	6	1.978E+06
2	9	5	1961	11	21	11	32	2.21E+04	14	8.334E+04
3	12	9	1961	8	12	8	29	1.78E+04	17	1.030E+05
4	26	4	1962	8	19	8	25	4.87E+08	4	1.254E+07
5	20	7	1962	8	24	8	38	5.57E+02	40	1.387E+04
6	31	8	1962	8	40	8	53	8.60E+03	30	1.347E+05
7	8	7	1963	8	17	8	25	3.49E+07	7	2.086E+07
8	14	10	1963	8	25	8	28	2.64E+06	12	6.117E+06
9	24	3	1964	13	38	13	49	8.09E+03	21	7.046E+04
10	28	4	1964	8	10	8	34	2.48E+03	31	4.205E+04
11	25	6	1964	8	54	9	6	5.92E-02	942	5.459E+01
12	11	10	1964	18	8	18	10	2.10E+09	7	1.255E+09
13	12	10	1964	17	58	18	1	3.24E+03	47	1.019E+05
14	17	6	1965	1	41	1	55	2.23E+04	19	1.479E+05
15	17	6	1965	9	28	9	40	7.97E+04	12	1.847E+05
16	3	9	1965	8	49	9	1	4.23E+01	83	2.784E+03
17	16	9	1965	8	46	9	3	1.48E+04	16	6.976E+04
18	17	9	1965	8	30	8	36	3.06E+06	7	1.487E+06
19	2	11	1965	0	41	1	2	9.54E+01	83	6.279E+03
20	27	11	1965	13	30	13	47	9.42E+06	7	4.579E+06
21	29	11	1965	0	47	0	53	4.46E-03	9870	4.393E+01
22	19	1	1966	1	23	1	32	8.62E+05	10	1.461E+06
23	3	2	1967	8	25	8	30	4.23E+04	15	1.725E+05
24	12	3	1967	8	25	8	28	9.33E+03	19	6.591E+04
25	7	5	1967	9	17	9	44	3.13E+06	6	1.217E+06
26	9	2	1968	8	31	8	45	1.46E+03	29	2.124E+04
27	15	3	1968	8	24	8	38	1.20E+05	13	3.615E+05
28	7	4	1968	8	49	9	25	2.58E+02	40	6.424E+03

Table A.1 (continued)

29	24	5	1968	13	34	13	51	3.33E+05	12	7.716E+05
30	10	6	1968	12	25	12	35	9.43E+04	10	1.261E+05
31	13	6	1968	8	20	8	41	9.32E+02	45	2.715E+04
32	7	7	1968	8	39	9	17	4.09E+00	182	6.669E+02
33	23	7	1968	8	59	9	29	1.33E+09	3	2.173E+07
34	8	8	1968	8	39	8	55	4.05E+03	22	3.778E+04
35	8	9	1968	8	55	9	7	2.89E+09	3	3.027E+07
36	13	9	1968	8	42	8	50	7.45E+04	11	1.577E+05
37	30	9	1968	8	15	8	53	3.51E+00	172	5.374E+02
38	30	9	1968	13	41	14	8	1.81E+04	15	7.380E+04
39	3	10	1968	8	21	8	42	1.83E+04	17	1.059E+05
40	31	10	1968	8	13	8	19	2.19E+02	45	6.380E+03
41	4	11	1968	7	56	8	6	4.84E+00	248	1.107E+03
42	28	1	1969	13	16	13	21	2.26E-02	1230	2.735E+01
43	16	3	1969	8	34	8	37	1.16E+01	124	1.224E+03
44	18	3	1969	8	17	8	20	2.48E+08	4	9.788E+06
45	8	9	1969	8	15	8	28	2.33E+03	50	7.897E+04
46	8	9	1969	11	29	11	53	2.41E+04	14	9.088E+04
47	10	10	1969	13	23	13	29	1.51E+09	3	1.582E+07
48	12	10	1969	8	18	8	23	6.35E+04	13	2.094E+05
49	2	3	1970	13	17	13	38	1.24E+02	74	7.075E+03
50	3	7	1970	8	43	9	49	4.91E+04	33	8.968E+05
51	29	7	1970	8	22	8	43	4.83E+04	23	4.846E+05
52	18	8	1970	8	53	9	22	1.24E+02	66	6.116E+03
53	26	8	1970	8	58	9	1	6.81E+07	4	4.052E+06
54	1	4	1971	8	40	8	46	1.03E+08	4	2.653E+06
55	2	7	1971	13	54	13	59	2.95E+05	12	6.835E+05
56	13	9	1971	8	11	8	19	1.95E+03	33	3.562E+04
57	18	9	1971	8	24	8	41	1.02E+05	13	3.363E+05
58	24	11	1971	8	22	8	29	1.10E+02	99	8.909E+03
59	17	12	1971	8	8	8	22	5.71E+01	88	4.031E+03
60	17	12	1971	13	2	13	19	1.18E-02	1230	1.428E+01
61	30	3	1972	1	22	1	41	7.30E+02	42	1.965E+04
62	15	4	1972	8	11	8	31	5.29E-03	1800	9.417E+00
63	18	4	1972	8	9	8	24	1.62E-03	3440	5.540E+00
64	16	9	1972	8	18	8	23	2.49E+04	19	1.759E+05
65	23	9	1972	13	37	13	48	6.51E+02	50	2.206E+04
66	29	9	1972	8	15	8	33	2.29E+03	29	3.332E+04
67	29	9	1972	13	22	13	28	8.88E-03	1680	1.474E+01
68	15	11	1972	12	53	13	14	6.84E-03	9020	6.156E+01
69	27	12	1972	12	50	13	18	3.44E-02	20800	7.148E+02
70	10	1	1973	13	7	13	18	1.05E-02	1740	1.806E+01
71	9	2	1973	8	8	8	23	5.23E-02	942	4.823E+01
72	25	2	1973	8	30	8	35	1.63E+08	3	2.663E+06
73	25	2	1973	10	22	10	24	2.62E+05	10	3.503E+05
74	3	3	1973	8	16	8	19	3.47E-01	350	1.147E+02
75	20	3	1973	8	15	8	39	7.21E+03	17	3.877E+04
76	25	3	1973	8	9	8	30	1.10E+03	36	2.351E+04
77	11	4	1973	8	34	8	40	8.63E+03	16	4.351E+04

Table A.1 (continued)

78	18	4	1973	8	7	8	31	4.52E+01	105	3.923E+03
79	19	4	1973	8	22	8	27	1.30E+04	27	1.749E+05
80	21	4	1973	8	15	8	41	2.67E+03	40	6.648E+04
81	21	4	1973	10	20	10	29	5.31E+03	21	4.625E+04
82	22	4	1973	8	21	8	38	3.34E+05	14	1.259E+06
83	22	4	1973	10	27	10	39	3.56E-01	350	1.177E+02
84	20	5	1973	8	41	8	55	9.01E+04	10	1.527E+05
85	23	5	1973	8	23	8	35	8.46E+03	18	5.190E+04
86	27	8	1973	8	29	8	38	6.65E+03	17	3.848E+04
87	28	8	1973	8	43	8	45	4.39E-03	6820	2.985E+01
88	3	10	1973	8	24	8	33	1.32E+06	10	2.237E+06
89	17	10	1973	8	29	8	40	4.77E+03	18	2.926E+04
90	20	10	1973	8	47	9	7	3.72E+04	14	1.403E+05
91	26	12	1974	13	52	14	24	8.45E-03	1320	1.099E+01
92	24	3	1974	8	31	9	24	5.10E-03	8820	4.488E+01
93	25	3	1974	8	27	8	33	2.11E+07	5	2.639E+06
94	1	4	1974	8	14	8	35	3.84E-03	2720	1.037E+01
95	1	4	1974	13	27	13	45	2.09E+02	45	6.088E+03
96	4	4	1974	8	17	8	37	2.83E+06	8	2.425E+06
97	4	4	1974	11	1	11	25	5.00E-01	288	1.343E+02
98	7	4	1974	8	37	8	46	6.22E+02	213	1.206E+05
99	20	4	1974	13	20	13	34	3.37E+04	13	1.111E+05
100	21	4	1974	8	13	8	48	2.29E+03	45	6.671E+04
101	25	4	1974	8	14	8	21	5.33E+03	21	4.318E+04
102	25	4	1974	13	16	13	31	8.73E-01	43400	3.787E+04
103	30	4	1974	8	25	8	38	9.62E+06	8	8.242E+06
104	24	5	1974	8	37	8	49	5.25E+06	6	1.215E+06
105	3	6	1974	13	8	13	17	1.78E+01	117	1.755E+03
106	27	6	1974	8	9	8	29	1.34E+05	16	6.316E+05
107	5	7	1974	8	23	8	43	1.54E+04	15	6.279E+04
108	14	7	1974	8	29	8	41	1.14E+04	17	6.597E+04
109	22	7	1974	8	23	8	29	6.28E+00	124	6.627E+02
110	24	7	1974	8	19	8	25	2.63E+04	18	1.613E+05
111	27	7	1974	8	24	8	33	1.01E+03	45	2.942E+04
112	21	8	1974	8	16	8	34	1.47E-01	529	7.488E+01
113	23	8	1974	8	20	8	32	8.72E-03	1860	1.605E+01
114	19	9	1974	8	27	8	32	6.23E+06	7	3.028E+06
115	20	9	1974	8	18	8	36	2.16E+03	36	4.616E+04
116	17	10	1974	8	26	8	54	1.87E+01	105	1.623E+03
117	20	10	1974	8	20	8	29	3.97E+03	35	7.847E+04
118	22	10	1974	8	15	8	32	2.09E+04	15	9.179E+04
119	24	10	1974	13	24	13	26	2.96E-03	2410	7.075E+00
120	26	10	1974	8	25	8	46	2.07E-01	30100	6.227E+03
121	14	1	1975	8	27	8	30	4.36E+09	3	4.567E+07
122	5	3	1975	8	13	8	27	1.98E+01	105	1.718E+03
123	11	3	1975	8	2	8	24	1.74E+03	42	4.683E+04
124	24	3	1975	13	29	13	44	1.71E+00	182	2.788E+02
125	9	4	1975	8	15	8	18	3.59E+03	36	7.672E+04
126	13	4	1975	8	21	8	27	3.79E+06	5	6.518E+05

Table A.1 (continued)

127	2	6	1975	8	33	8	45	1.03E+12	2	2.939E+09
128	8	7	1975	13	27	13	38	4.14E+08	4	1.066E+07
129	10	7	1975	8	23	8	39	3.89E+04	12	9.817E+04
130	11	7	1975	8	22	8	37	3.10E+04	14	1.095E+05
131	5	8	1975	13	3	13	6	9.34E+00	303	2.649E+03
132	6	8	1975	8	44	8	49	4.81E+08	3	3.250E+06
133	10	8	1975	8	21	8	48	1.66E+04	21	1.345E+05
134	14	8	1975	8	32	9	0	7.60E+06	7	4.543E+06
135	20	8	1975	13	25	13	31	1.75E+07	5	3.010E+06
136	30	8	1975	8	37	8	43	9.11E+07	4	2.347E+06
137	9	10	1975	8	21	8	30	1.14E+08	6	3.459E+07
138	31	10	1975	8	47	8	56	1.27E+10	2	4.147E+07
139	4	11	1975	8	37	8	42	3.84E+11	2	9.806E+08
140	6	11	1975	13	29	13	32	2.10E+10	3	1.419E+08
141	1	12	1975	8	23	8	37	1.66E+05	12	3.846E+05
142	27	12	1975	8	15	8	30	3.43E+04	20	2.600E+05
143	21	1	1976	13	13	13	20	3.17E+02	45	9.235E+03
144	10	2	1976	8	26	8	35	5.68E+04	11	1.203E+05
145	8	3	1976	8	12	8	34	2.14E+04	23	2.147E+05
146	8	3	1976	12	15	12	36	5.29E+05	10	8.041E+05
147	28	3	1976	8	28	8	35	1.96E+06	7	1.172E+06
148	29	3	1976	8	22	8	36	1.55E+07	6	6.027E+06
149	3	4	1976	8	21	8	34	3.72E+03	35	7.353E+04
150	4	4	1976	8	4	8	22	9.50E-03	1920	1.805E+01
151	6	4	1976	8	6	8	33	1.21E+01	155	1.648E+03
152	4	7	1976	8	46	9	0	2.76E+10	3	1.865E+08
153	16	7	1976	8	26	8	29	5.83E+04	17	3.135E+05
154	30	7	1976	8	42	9	14	1.12E+03	26	1.395E+04
155	30	7	1976	13	41	13	47	1.52E+09	2	3.882E+06
156	2	9	1976	8	2	8	20	2.13E-03	4300	9.116E+00
157	20	9	1976	8	10	8	25	3.13E+03	30	4.901E+04
158	17	10	1976	8	17	8	47	7.63E+01	79	4.680E+03
159	18	10	1976	8	22	8	28	4.54E+04	15	1.851E+05
160	18	11	1976	13	38	13	40	6.94E+00	248	1.588E+03
161	9	3	1977	8	18	8	24	6.80E+03	16	3.429E+04
162	6	4	1977	8	34	8	51	1.99E+06	5	2.489E+05
163	7	4	1977	8	31	8	54	2.34E+03	21	2.038E+04
164	9	4	1977	8	20	8	25	2.85E+04	14	1.075E+05
165	14	7	1977	13	51	13	54	5.15E+05	7	3.079E+05
166	29	7	1977	8	35	8	49	1.05E+04	14	3.959E+04
167	30	7	1977	8	40	8	49	4.05E+06	6	1.575E+06
168	7	8	1977	8	43	8	59	3.60E+06	7	1.750E+06
169	11	8	1977	8	39	8	44	4.87E+08	4	1.254E+07
170	17	8	1977	8	41	8	53	6.11E+04	11	1.176E+05
171	27	9	1977	8	41	8	51	7.14E+06	5	8.929E+05
172	4	4	1978	6	53	7	4	1.61E+05	9	1.621E+05
173	24	4	1978	7	18	7	26	6.53E+04	12	1.513E+05
174	26	4	1978	7	41	8	15	1.42E+02	70	7.538E+03
175	3	5	1978	7	4	7	25	2.43E+05	13	7.320E+05

Table A.1 (continued)

176	24	6	1978	6	42	7	6	7.67E+00	131	8.625E+02
177	12	8	1978	7	11	7	20	1.46E+10	2	3.728E+07
178	30	8	1978	7	4	7	15	7.18E+03	21	5.817E+04
179	28	9	1978	7	5	7	10	6.10E+07	5	5.366E+06
180	30	9	1978	6	59	7	14	1.44E+05	10	1.926E+05
181	22	10	1978	6	59	7	24	1.30E+04	19	9.184E+04
182	27	10	1978	7	15	7	24	3.47E+05	8	2.503E+05
183	28	10	1978	6	51	7	9	9.95E+04	13	3.281E+05
184	26	11	1978	6	43	7	4	1.12E+01	182	1.826E+03
185	4	12	1979	7	2	7	16	3.24E+04	19	2.289E+05
186	4	1	1979	6	45	6	56	6.38E+04	15	2.802E+05
187	26	2	1979	12	57	13	18	7.81E+05	9	7.865E+05
188	27	2	1979	6	59	7	29	1.31E+02	53	4.798E+03
189	17	4	1979	7	12	7	26	8.24E+03	17	4.768E+04
190	2	5	1979	7	10	7	23	1.10E+06	7	5.347E+05
191	19	8	1979	7	7	7	15	1.88E+04	13	5.663E+04
192	9	10	1979	12	53	13	7	3.64E+04	14	1.373E+05
193	14	11	1979	7	27	7	47	9.95E+04	10	1.330E+05
194	11	4	1980	7	47	8	17	1.98E-02	1180	2.297E+01
195	16	4	1980	7	6	7	11	3.25E+05	9	3.273E+05
196	13	6	1980	6	53	7	11	5.62E+03	23	5.639E+04
197	25	10	1980	13	14	13	17	6.39E+07	4	3.802E+06
198	14	4	1981	7	52	8	13	1.69E+05	10	2.569E+05
199	7	6	1981	7	48	8	11	7.09E+04	13	1.979E+05
200	29	6	1981	7	56	8	2	6.94E+03	31	1.177E+05
201	26	7	1981	8	2	8	13	1.44E+08	4	8.568E+06
202	5	8	1981	7	45	7	53	4.38E-02	837	3.579E+01
203	3	10	1981	7	4	7	25	1.61E+08	5	1.416E+07
204	18	11	1981	6	57	7	3	7.36E+06	5	9.204E+05
205	28	1	1982	12	56	13	2	2.40E+08	4	6.182E+06
206	4	2	1982	7	6	7	12	6.30E+05	7	3.766E+05
207	5	2	1982	6	50	7	7	1.07E+04	17	5.753E+04
208	13	2	1982	6	52	7	12	9.56E+04	14	3.376E+05
209	6	4	1982	7	56	7	58	5.43E+05	9	6.325E+05
210	14	7	1982	7	50	7	53	1.19E+08	6	3.611E+07
211	29	7	1982	14	2	14	4	1.87E+06	8	1.602E+06
212	31	7	1982	7	52	8	7	2.95E+03	24	3.171E+04
213	25	8	1982	7	47	8	2	4.29E+03	23	4.304E+04
214	25	8	1982	13	45	13	51	5.54E+03	19	3.674E+04
215	30	8	1982	7	53	7	59	7.47E+03	18	4.583E+04
216	3	9	1982	8	5	8	9	7.05E+07	4	4.195E+06
217	5	9	1982	8	9	8	19	1.26E+09	3	8.513E+06
218	5	9	1982	10	30	10	49	3.48E+04	14	1.229E+05
219	7	9	1982	8	6	8	15	9.01E+05	6	3.504E+05
220	7	2	1983	6	57	7	14	8.83E+05	12	2.046E+06
221	18	1	1983	6	54	7	15	2.04E+01	111	1.891E+03
222	8	2	1983	7	10	7	21	1.96E+07	5	1.724E+06
223	18	2	1983	6	54	7	14	1.50E+02	47	4.719E+03
224	20	3	1983	6	47	7	2	4.32E+02	38	9.971E+03

Table A.1 (continued)

225	1	4	1983	7	54	8	13	6.47E+04	14	2.440E+05
226	2	4	1983	8	0	8	12	1.07E+00	191	1.841E+02
227	8	4	1983	8	8	8	26	3.11E+05	8	2.665E+05
228	15	4	1983	7	55	8	3	8.57E+05	8	7.343E+05
229	22	4	1983	8	4	8	21	7.02E+03	13	2.315E+04
230	26	4	1983	8	8	8	32	3.69E+05	8	3.162E+05
231	6	5	1983	8	0	8	21	3.67E+04	13	1.106E+05
232	12	5	1983	7	50	7	56	1.05E+06	8	8.996E+05
233	12	5	1983	13	54	14	9	1.03E+01	117	1.016E+03
234	14	5	1983	7	47	8	14	2.16E+03	33	3.945E+04
235	15	5	1983	13	59	14	8	1.20E+04	18	7.362E+04
236	21	6	1983	7	56	8	19	4.54E+01	70	2.410E+03
237	13	7	1983	8	25	8	33	1.94E+06	6	5.887E+05
238	2	8	1983	7	33	8	18	7.14E-03	1920	1.357E+01
239	12	8	1983	8	15	8	23	1.14E+10	2	3.723E+07
240	23	8	1983	7	54	8	23	3.60E+03	21	3.136E+04
241	24	8	1983	8	6	8	20	1.98E+05	10	2.648E+05
242	25	8	1983	10	5	10	12	5.74E+04	10	9.729E+04
243	26	8	1983	7	57	8	17	3.26E-02	942	3.006E+01
244	31	8	1983	7	48	8	2	9.22E+04	13	2.777E+05
245	16	9	1983	8	7	8	20	3.20E+06	6	7.406E+05
246	17	9	1983	7	48	8	16	2.82E+00	213	5.468E+02
247	26	9	1983	8	15	8	25	2.63E+08	3	4.296E+06
248	3	10	1983	6	46	7	3	4.38E+07	5	7.532E+06
249	14	10	1983	7	9	7	29	1.39E+06	6	5.405E+05
250	29	10	1983	6	49	7	0	1.58E+04	21	1.280E+05
251	5	1	1984	6	47	6	49	2.08E+05	16	9.804E+05
252	14	2	1984	6	27	6	30	2.07E+06	8	1.774E+06
253	23	2	1984	6	59	7	16	4.35E+03	17	2.517E+04
254	2	3	1984	8	0	8	12	2.46E+04	12	6.208E+04
255	3	3	1984	6	41	7	18	1.11E+03	40	2.764E+04
256	7	3	1984	6	47	7	14	1.07E+02	56	4.223E+03
257	19	3	1984	6	51	7	3	1.12E+06	7	5.444E+05
258	30	3	1984	6	48	7	8	1.60E+04	26	1.993E+05
259	5	4	1984	7	59	8	20	8.28E+03	16	3.903E+04
260	20	4	1984	7	51	8	11	8.31E+00	191	1.429E+03
261	2	5	1984	8	5	8	19	3.82E+03	21	3.327E+04
262	6	5	1984	7	59	8	2	8.95E+03	14	3.375E+04
263	19	5	1984	8	3	8	11	1.80E+06	5	2.251E+05
264	20	5	1984	7	59	8	10	5.43E+00	124	5.730E+02
265	21	5	1984	7	45	8	9	3.58E+03	21	3.118E+04
266	22	5	1984	7	56	8	28	1.69E+04	18	1.037E+05
267	23	5	1984	8	12	8	14	6.60E+08	2	1.782E+06
268	17	7	1984	7	44	8	11	6.68E-03	1860	1.229E+01
269	28	7	1984	8	8	8	11	5.60E+03	16	2.824E+04
270	20	8	1984	8	4	8	25	3.15E+05	13	8.792E+05
271	27	8	1984	13	52	14	13	1.68E+05	13	5.539E+05
272	28	8	1984	14	18	14	24	9.96E+05	8	8.533E+05
273	5	9	1984	7	59	8	10	2.53E+05	13	7.621E+05

Table A.1 (continued)

274	20	9	1984	8	11	8	28	4.18E+04	13	1.167E+05
275	23	9	1984	8	10	8	18	5.26E+05	11	1.114E+06
276	24	9	1984	7	55	8	18	1.77E+05	15	7.217E+05
277	26	9	1984	7	52	8	25	7.63E+04	15	3.111E+05
278	27	9	1984	13	57	14	18	1.85E+06	9	1.863E+06
279	10	10	1984	7	14	7	23	1.26E+04	14	4.751E+04
280	19	10	1984	6	51	7	2	3.39E+01	131	3.812E+03
281	20	10	1984	6	57	7	18	1.26E+02	59	5.369E+03
282	22	10	1984	7	9	7	23	4.50E+07	5	5.628E+06
283	23	10	1984	7	18	7	21	1.82E+05	10	3.085E+05
284	24	10	1984	6	45	6	59	1.27E+03	40	3.162E+04
285	25	10	1984	13	16	13	21	2.39E+08	4	9.433E+06
286	20	11	1984	6	59	7	13	1.19E+00	202	2.177E+02
287	3	12	1984	9	3	9	18	1.40E-01	462	6.194E+01
288	11	1	1985	7	4	7	19	2.88E+06	7	1.400E+06
289	25	4	1985	7	38	8	11	7.67E-01	484	3.562E+02
290	27	4	1985	8	3	8	35	2.48E+07	5	4.265E+06
291	29	4	1985	7	49	8	16	8.50E-01	288	2.284E+02
292	14	8	1985	7	45	7	57	4.91E+03	25	5.715E+04
293	21	9	1985	7	35	8	8	8.59E+00	213	1.666E+03
294	9	10	1985	6	59	7	5	4.85E+04	15	2.130E+05
295	15	10	1985	7	1	7	41	1.22E+07	5	1.526E+06
296	22	2	1986	6	47	7	7	1.23E+04	22	1.147E+05
297	7	3	1986	6	51	7	0	1.20E+04	16	5.656E+04
298	25	3	1986	6	56	7	23	2.13E+02	38	4.916E+03
299	10	4	1986	7	52	8	15	1.52E+03	25	1.769E+04
300	6	5	1986	8	10	8	46	1.96E+05	14	6.921E+05
301	28	6	1986	7	57	8	3	1.62E+04	14	6.109E+04
302	23	8	1986	6	45	7	9	1.42E+03	31	2.408E+04
303	25	8	1986	7	5	7	25	3.03E+04	14	1.070E+05
304	19	9	1986	7	39	7	51	1.34E+09	2	3.824E+06
305	23	9	1986	7	19	7	38	7.03E+08	3	7.364E+06
306	27	9	1986	6	58	7	22	4.13E+05	9	4.811E+05
307	4	11	1986	7	9	7	30	3.51E+05	8	3.007E+05
308	5	11	1986	7	1	7	41	6.31E+05	10	9.591E+05
309	25	5	1987	7	46	7	51	3.33E+08	2	8.504E+05
310	27	5	1987	7	19	7	34	1.28E+06	5	2.201E+05
311	26	8	1987	13	11	13	28	4.60E+04	11	8.855E+04
312	2	9	1987	6	29	6	59	4.30E+03	25	5.005E+04
313	12	9	1987	7	5	7	22	1.37E+02	53	5.017E+03
314	26	9	1987	7	6	7	24	9.14E+04	11	1.935E+05
315	27	10	1987	7	13	7	24	1.29E+07	5	1.135E+06
316	5	2	1988	7	29	7	52	7.85E+04	10	1.193E+05
317	12	2	1988	7	9	7	41	1.69E+06	6	6.572E+05
318	23	2	1988	6	56	7	17	4.42E+04	15	1.941E+05
319	30	3	1988	7	11	7	22	1.35E+07	4	5.328E+05
320	2	4	1988	6	30	7	3	8.02E+04	12	1.858E+05
321	6	4	1988	7	25	7	42	3.25E+09	2	8.299E+06
322	21	5	1988	7	4	7	13	1.08E+04	18	6.626E+04

Table A.1 (continued)

323	20	6	1988	6	57	7	33	3.30E-03	1860	6.072E+00
324	3	11	1988	6	49	7	3	2.09E+07	5	1.838E+06
325	27	12	1988	6	43	6	45	2.49E+04	17	1.441E+05
326	17	3	1989	6	38	6	56	1.59E+08	4	6.276E+06
327	19	3	1989	7	9	7	15	8.00E+04	11	1.540E+05
328	22	3	1989	6	59	7	18	1.70E+06	6	6.611E+05
329	28	3	1989	7	3	7	12	3.83E+06	5	4.790E+05
330	7	4	1989	6	49	7	18	4.26E+08	3	6.959E+06
331	20	4	1989	7	3	7	32	5.60E+04	10	9.492E+04
332	10	6	1989	6	57	7	33	2.61E+07	7	1.560E+07
333	1	3	1990	7	11	7	35	8.60E+04	10	1.307E+05
334	6	3	1990	6	53	7	23	1.98E+03	23	1.987E+04
335	23	3	1990	6	57	7	15	7.14E+04	11	1.512E+05
336	11	4	1990	7	8	7	26	3.63E-02	683	2.408E+01
337	13	4	1990	7	45	7	48	4.36E+10	3	4.218E+08
338	14	4	1990	7	12	7	27	1.28E+05	12	2.966E+05
339	27	4	1990	7	45	7	47	6.04E+05	6	2.349E+05
340	28	4	1990	7	9	7	21	1.34E+04	14	5.053E+04
341	10	5	1990	9	28	9	37	1.19E+05	11	2.520E+05
342	21	8	1990	4	34	5	1	9.88E+03	18	6.061E+04
343	22	8	1990	3	55	3	58	4.80E+00	191	8.257E+02
344	31	8	1990	4	11	4	29	4.76E+04	10	8.068E+04
345	19	9	1990	6	50	7	5	3.46E+03	26	4.311E+04
346	2	5	1991	9	10	9	22	3.28E+08	3	2.216E+06
347	2	9	1991	7	54	8	18	6.85E+03	30	1.073E+05
348	17	2	1993	6	46	6	48	9.29E+07	12	2.153E+08
349	15	3	1993	7	40	7	57	6.92E+05	9	8.060E+05
350	29	3	1993	7	12	7	16	3.04E+10	2	8.209E+07
351	21	4	1993	7	50	8	11	1.37E+01	105	1.189E+03
352	2	12	1993	7	12	7	36	4.21E+02	56	1.662E+04
353	19	1	1994	7	5	7	20	2.08E+00	261	5.028E+02
354	20	1	1994	8	59	9	2	1.52E+02	93	1.149E+04
355	26	1	1994	7	53	8	41	3.60E-02	979	3.453E+01
356	27	1	1994	8	21	8	27	2.15E+07	7	1.045E+07
357	28	1	1994	7	1	7	37	3.76E+01	88	2.655E+03
358	7	2	1994	6	58	7	16	2.86E+02	56	1.129E+04
359	8	2	1994	7	33	7	50	2.61E-03	4660	1.211E+01
360	8	3	1994	7	5	7	40	2.52E+01	111	2.336E+03
361	11	3	1994	6	59	7	29	1.27E+04	22	1.185E+05
362	15	3	1994	6	59	7	14	8.90E+05	16	4.195E+06
363	15	3	1994	7	17	7	35	1.15E+02	117	1.134E+04
364	4	4	1994	6	58	7	10	1.54E+02	63	7.063E+03
365	5	4	1994	6	55	7	28	1.20E+03	36	2.564E+04
366	7	4	1994	7	1	7	49	4.01E+02	53	1.469E+04
367	8	4	1994	6	41	6	44	1.85E-02	6650	1.227E+02
368	11	4	1994	6	49	7	37	2.30E-01	577	1.282E+02
369	12	4	1994	7	35	8	0	2.56E+08	3	1.164E+06
370	2	5	1994	7	17	7	26	4.78E+07	5	4.205E+06
371	3	5	1994	6	41	7	11	2.29E-01	422	9.216E+01

Table A.1 (continued)

372	4	5	1994	7	17	7	34	2.12E+06	8	1.529E+06
373	5	5	1994	7	19	7	31	7.50E+04	13	2.093E+05
374	6	5	1994	7	21	7	54	1.32E+07	6	4.005E+06
375	7	5	1994	6	49	7	10	1.89E+01	117	1.864E+03
376	10	5	1994	6	59	7	58	3.70E+04	24	3.978E+05
377	13	5	1994	7	28	8	4	1.51E+03	31	2.560E+04
378	17	5	1994	7	14	7	28	7.68E+06	5	6.755E+05
379	24	5	1994	7	36	8	6	4.86E+04	13	1.602E+05
380	31	5	1994	6	43	7	19	8.69E+03	23	8.719E+04
381	1	6	1994	7	22	7	28	9.73E+00	99	7.880E+02
382	13	9	1994	6	52	7	22	2.62E-02	22000	5.759E+02
383	5	10	1994	7	1	7	22	3.97E+02	42	1.069E+04
384	6	10	1994	6	49	7	22	9.13E-02	837	7.461E+01
385	29	10	1994	7	23	7	50	3.75E+03	23	3.763E+04
386	31	10	1994	7	22	7	37	8.12E+08	4	3.205E+07
387	2	3	1995	6	54	7	21	7.32E+02	35	1.447E+04
388	28	3	1995	6	47	7	20	7.05E-02	529	3.591E+01
389	24	4	1995	6	25	7	1	7.52E+02	42	2.024E+04
390	4	5	1995	7	4	7	34	3.44E+02	66	1.697E+04
391	6	5	1995	8	54	9	33	9.52E+06	7	4.628E+06
392	31	5	1995	7	52	8	27	2.60E+01	105	2.257E+03
393	19	6	1995	7	5	7	16	2.93E+05	9	3.413E+05
394	27	9	1995	8	17	8	40	8.00E+03	22	7.462E+04
395	6	10	1995	6	21	6	48	3.77E-03	4420	1.659E+01
396	9	10	1995	7	43	8	13	9.53E+02	40	2.373E+04
397	19	10	1995	7	33	7	42	5.51E+04	14	1.946E+05
398	2	11	1995	7	7	7	46	6.44E-03	2050	1.307E+01
399	6	11	1995	6	58	7	15	1.15E+06	8	8.296E+05
400	2	12	1995	3	58	4	3	3.96E+08	8	2.857E+08
401	4	12	1995	9	16	9	42	1.82E+04	14	6.863E+04
402	25	2	1996	7	29	7	41	1.30E+04	18	7.975E+04
403	17	4	1996	10	39	10	48	1.42E+10	2	4.637E+07
404	18	4	1996	7	16	7	34	5.75E+02	40	1.432E+04
405	19	4	1996	8	4	8	28	6.22E+04	16	3.136E+05
406	28	6	1996	4	48	4	55	7.85E+05	13	2.588E+06
407	3	7	1996	6	38	6	50	2.33E+04	19	1.545E+05
408	7	7	1996	7	12	7	30	2.69E+02	59	1.146E+04
409	30	8	1996	7	3	7	30	4.13E+07	4	1.630E+06
410	7	9	1996	9	53	10	20	1.55E+03	27	2.086E+04
411	14	9	1996	8	29	8	56	2.83E+06	5	4.867E+05
412	23	10	1996	8	7	8	40	1.13E+00	248	2.585E+02
413	4	11	1996	10	58	11	5	1.91E+08	3	2.001E+06
414	28	2	1997	7	8	7	44	2.34E+03	29	3.405E+04
415	11	4	1997	7	49	8	15	3.37E+04	14	1.271E+05
416	18	4	1997	8	4	8	22	1.22E+09	3	5.549E+06
417	11	7	1997	8	27	8	39	1.11E+10	2	3.168E+07
418	28	9	1997	6	53	7	32	1.21E+07	7	7.233E+06
419	10	10	1997	6	51	7	8	6.58E+02	42	1.771E+04
420	17	11	1997	7	26	7	32	1.04E+02	99	8.423E+03

Table A.1 (continued)

421	23	11	1997	7	50	8	17	4.11E+04	15	1.805E+05
422	27	11	1997	8	58	9	43	1.81E+05	10	2.751E+05
423	1	12	1997	9	19	9	46	9.53E+08	4	3.761E+07
424	11	12	1997	7	59	8	2	8.26E+11	2	2.697E+09
425	13	12	1997	12	1	12	43	1.50E+01	124	1.583E+03
426	31	12	1997	8	32	8	49	1.27E+08	6	3.854E+07
427	8	5	1998	8	32	8	56	4.66E+06	9	4.693E+06
428	26	6	1998	7	54	8	15	1.95E+08	5	1.715E+07
429	24	8	1998	8	32	8	59	1.56E+05	9	1.571E+05
430	28	8	1998	8	9	8	45	6.24E+04	13	1.880E+05
431	31	8	1998	7	58	8	13	2.13E+08	3	9.688E+05
432	9	10	1998	7	44	8	17	1.99E+08	6	7.738E+07
433	13	11	1998	7	54	8	21	2.43E+06	11	5.145E+06
434	25	11	1998	8	18	8	24	5.15E+06	10	6.886E+06
435	27	11	1998	7	34	7	52	1.96E+04	18	1.202E+05
436	12	2	1999	9	45	10	23	5.92E+03	22	5.522E+04
437	19	2	1999	7	31	8	3	1.15E+04	29	1.673E+05
438	15	3	1999	7	34	8	3	2.04E+06	6	6.190E+05
439	13	9	1999	8	36	9	6	2.84E+02	53	1.040E+04
440	15	9	1999	7	50	8	23	3.57E+00	202	6.532E+02
441	28	9	1999	8	14	8	32	6.10E+06	10	9.272E+06
442	29	9	1999	8	19	9	10	5.15E+06	8	3.715E+06
443	11	10	1999	8	25	9	4	6.54E+02	56	2.581E+04
444	8	11	1999	8	38	9	5	3.66E+05	10	5.563E+05
445	3	12	1999	8	35	8	38	3.23E+10	5	4.039E+09
446	6	12	1999	7	54	8	30	3.67E+00	213	7.117E+02
447	13	12	1999	8	39	8	46	9.27E+09	3	1.514E+08
448	6	3	2000	8	48	9	21	9.58E+09	2	3.128E+07
449	5	5	2000	8	44	9	28	1.64E+02	70	8.706E+03
450	10	7	2000	9	15	9	27	1.48E+05	11	2.849E+05
451	1	9	2000	7	35	8	35	2.08E+09	2	5.312E+06
452	26	1	2001	7	32	8	14	8.40E+01	93	6.350E+03
453	5	3	2001	8	7	8	12	2.39E+08	4	6.156E+06
454	21	3	2001	7	54	8	0	6.35E+05	9	7.397E+05
455	9	4	2001	9	16	9	37	2.61E+10	2	8.523E+07
456	18	7	2001	9	16	9	25	1.89E+05	12	4.770E+05
457	27	7	2001	9	4	9	34	2.15E+04	17	1.156E+05
458	3	8	2001	8	25	8	40	4.91E+07	4	1.938E+06
459	12	9	2001	8	58	9	34	5.33E+07	11	9.91E+07
460	8	3	2002	9	8	9	50	1.27E+03	7	7.99E+02
461	22	7	2002	10	38	11	5	7.87E+07	3	1.286E+06
462	16	8	2002	10	16	10	37	1.37E+04	14	4.838E+04
463	19	8	2002	9	50	10	5	3.96E+05	6	1.202E+05
464	21	8	2002	10	18	10	24	2.00E+10	4	5.152E+08
465	11	9	2002	10	7	10	25	7.70E+08	4	4.27E+07
466	7	10	2002	9	32	10	23	7.77E+02	117	7.65E+04
467	9	10	2002	9	45	10	18	1.92E+06	16	9.68E+06
468	21	10	2002	9	47	10	11	1.21E+07	9	1.57E+07
469	30	10	2002	8	35	9	17	9.37E+01	309	2.71E+04

Table A.1 (continued)

470	13	1	2003	9	21	9	54	3.81E+04	26	4.75E+05
471	17	1	2003	10	2	10	59	1.03E+06	12	2.69E+06
472	31	1	2003	8	50	9	29	3.85E+02	140	4.67E+04
473	10	2	2003	9	1	9	28	2.05E+03	87	1.43E+05
474	17	3	2003	8	40	8	46	8.02E+06	20	6.08E+07
475	4	4	2003	10	30	10	51	1.23E+06	17	6.49E+06
476	25	4	2003	9	22	9	43	2.51E+09	6	5.85E+08
477	2	5	2003	9	31	9	52	8.48E+07	7	3.81E+07
478	7	5	2003	9	26	9	35	6.10E+07	10	9.272E+07
479	7	7	2003	8	55	9	37	1.84E+02	285	4.87E+04
480	11	7	2003	9	11	9	44	7.86E+03	91	5.75E+05
481	30	7	2003	9	28	9	55	2.65E+06	17	1.425E+07
482	8	8	2003	9	44	10	2	3.10E+10	3	1.410E+08
483	22	8	2003	9	53	10	17	1.61E+10	5	2.89E+09
484	25	8	2003	8	57	9	33	3.17E+03	83	2.086E+05
485	17	9	2003	9	19	9	46	1.28E+11	3	8.648E+08
486	19	9	2003	8	56	9	2	3.27E+10	8	2.359E+10
487	19	9	2003	9	5	9	11	3.40E+00	1990	6.698E+03
488	22	9	2003	9	43	10	7	2.06E+09	7	1.001E+09
489	26	9	2003	9	12	9	33	5.73E+07	8	3.75E+07
490	26	9	2003	9	12	9	57	5.78E+05	19	3.95E+06
491	15	10	2003	8	26	9	11	1.84E+01	455	8.01E+03
492	17	10	2003	8	44	8	53	3.16E+08	11	6.083E+08
493	17	10	2003	8	53	9	7	1.03E+00	2260	2.307E+03
494	22	10	2003	8	49	9	37	2.32E+03	94	1.77E+05
495	14	11	2003	8	43	9	25	2.80E-01	2680	7.47E+02
496	7	1	2004	8	29	8	59	4.96E-01	5450	2.69E+03
497	9	1	2004	8	50	9	5	2.84E+05	19	2.06E+06
498	13	3	2004	8	44	9	14	1.35E+03	163	1.94E+05
499	9	4	2004	9	45	10	9	2.95E+01	456	1.29E+04
500	12	4	2004	10	2	10	20	5.49E+01	320	1.65E+04
501	16	4	2004	9	54	10	6	4.67E+03	93	3.54E+05
502	13	10	2004	9	53	10	14	8.71E+05	15	3.69E+06
503	9	2	2005	8	33	8	51	1.86E+06	16	9.22E+06
504	7	3	2005	8	25	8	43	5.16E+05	23	5.31E+06
505	13	5	2005	8	13	8	49	9.52E+03	63	4.42E+05
506	15	6	2005	8	3	8	24	3.25E+06	13	9.98E+06
507	18	7	2005	9	16	9	46	2.71E+01	466	1.21E+04
508	16	12	2005	9	9	9	24	1.56E+07	14	5.66E+07
509	10	4	2006	10	16	10	49	1.98E+02	293	5.43E+04
510	28	6	2006	10	7	10	16	4.49E+04	36	9.51E+05
511	7	8	2006	9	47	10	5	1.16E+06	19	8.06E+06
512	28	9	2009	8	23	8	35	1.87E+04	71	1.00E+06
513	31	3	2010	9	8	9	17	4.72E+02	196	8.35E+04
514	17	12	2010	12	33	12	45	2.84E+04	134	3.27E+06
515	25	7	2011	13	12	13	24	4.52E+03	71	2.45E+05
516	16	3	2012	13	5	13	17	4.00E+05	31	6.68E+06
517	23	11	2012	12	37	12	58	1.26E+06	67	6.29E+07
518	27	3	2013	12	57	13	12	1.11E+00	11800	1.30E+04

Table A.1 (continued)

519	19	7	2013	13	26	13	41	4.43E+05	18	2.66E+06
520	21	8	2013	13	34	13	49	1.19E+04	63	5.54E+05
521	21	8	2013	13	52	14	16	9.22E+00	576	5.13E+03
522	18	10	2013	13	3	13	18	1.09E+05	36	2.34E+06
523	25	10	2013	12	46	13	1	5.04E+03	82	3.28E+05
524	26	2	2014	13	9	13	24	1.04E+04	68	5.28E+05

Norilsk

N	Date			T ₀ -T _e (UT)				A _e	E ₀ , keV	J(E>20 keV)
1	4	6	1975	11	33	12	5	9.73E+02	24	1.05E+04
2	10	10	1975	11	12	11	45	1.16E+01	155	1.58E+03
3	30	7	1976	11	25	11	33	1.07E+03	36	2.29E+04
4	9	3	1977	10	25	10	51	1.05E+03	38	2.41E+04
5	4	4	1977	11	10	11	31	2.09E+00	172	3.20E+02
6	1	7	1977	10	51	11	0	1.19E+02	53	4.37E+03
7	19	7	1977	11	4	11	15	2.63E+03	24	2.84E+04
8	27	7	1977	11	2	11	7	4.29E+05	10	6.50E+05
9	26	9	1979	10	56	11	18	1.47E+01	99	1.19E+03
10	8	2	1982	11	3	11	17	3.65E-02	712	2.53E+01

Mirny

N	Date			T ₀ -T _e (UT)				A _e	E ₀ , keV	J(E>20 keV)
1	14	4	1966	8	19	8	30	1.94E+02	45	5.63E+03
2	30	6	1966	8	24	8	48	1.58E+02	88	1.12E+04
3	3	2	1967	8	16	8	34	7.04E+01	79	4.32E+03
4	15	7	1980	11	58	12	39	8.14E-03	6030	4.89E+01
5	3	4	1984	4	18	4	27	1.13E+06	21	9.18E+06
6	27	4	1984	4	29	4	42	3.30E+04	18	2.04E+05
7	21	5	1988	8	57	9	12	8.00E-01	37200	2.97E+04
8	13	8	1989	4	59	5	38	4.36E-02	2260	9.75E+01
9	1	12	1989	4	20	4	51	8.82E-01	367	3.07E+02
10	6	9	2000	4	17	4	23	9.56E+08	4	5.72E+07

Tixie Bay

N	Date			T ₀ -T _e (UT)				A _e	E ₀ , keV	J(E>20 keV)
1	31	3	1978	15	46	16	10	4.94E+05	9	5.76E+05
2	4	4	1978	5	39	5	48	2.87E+04	14	1.01E+05
3	3	5	1978	15	41	15	53	2.51E+10	3	2.61E+08
4	23	2	1979	7	4	7	19	1.12E-02	5310	5.95E+01

Table A.1 (continued)

5	11	3	1979	16	49	16	53	3.43E+04	21	2.99E+05
6	28	3	1979	2	45	3	15	8.71E-03	13600	1.18E+02
7	29	3	1979	4	48	4	56	1.88E+07	5	2.35E+06
8	8	9	1979	8	47	8	50	5.58E+06	7	3.34E+06
9	13	6	1980	3	7	3	10	5.28E+11	3	5.13E+09
10	15	4	1983	2	4	2	6	9.53E+07	9	9.59E+07
11	26	8	1983	7	16	7	21	1.78E+00	236	3.86E+02
12	17	9	1983	3	12	3	14	1.25E+05	10	1.89E+05
13	29	3	1984	19	2	19	11	8.31E+02	27	1.12E+04
14	12	4	1984	16	10	16	19	1.94E+04	19	1.37E+05
15	23	5	1984	6	17	6	23	3.80E+04	12	8.83E+04
16	25	8	1986	7	39	7	42	3.51E+05	12	8.94E+05
17	26	9	1986	7	34	7	46	1.24E+08	4	3.20E+06

2013–2015 and by the Program “Specification of ionization sources affecting atmospheric processes” led by Irina Mironova.

Appendix

See Table A1

References

- Agostinelli, S., Allison, J., Amakoe, K., et al., 2003. Geant4 – a simulation toolkit. *Nucl. Instrum. Methods Phys. Res. Sect. A: Accl. Spectrom. Detect. Assoc. Equip.* 506, 250–303.
- Bazilevskaya, G.A., Svirzhevskaya, A.K., 1998. On the stratospheric measurements of cosmic rays. *Space Sci. Rev.* 85, 431–521.
- Bazilevskaya, G.A., Krainev, M.B., Stozhkov, Yu.I., Svirzhevskaya, A.K., Svirzhevsky, N.S., 1991. Long-term Soviet program for the measurement of ionizing radiation in the atmosphere. *J. Geomagn. Geoelectr.* 43, 893–900.
- Bazilevskaya, G.A., Makhmutov, V.S., Svirzhevskaya, A.K., Svirzhevsky, N.S., Stozhkov, Yu.I., Vashenyuk, E.V., 2002. Intrusion of energetic electrons into the polar atmosphere during the solar proton event of 24 September, 2001. *Physics of Auroral Phenomena*. In: Proceedings of XXV Annual Seminar, Apatity, Kola Science Center, RAS, Polar Geophys. Institute, 125–128.
- Berger, M.J., Seltzer, S.M., 1972. Bremsstrahlung in the atmosphere. *J. Atmos. Sol. Terr. Phys.* 34, 85–108.
- Berger, M.J., Seltzer, S.M., Maeda, K., 1974. Some new results on electron transport in the atmosphere. *J. Atmos. Terr. Phys.* 36, 591–601.
- Blake, J.B., Looper, M.D., Baker, D.N., Nakamura, R., Kleker, B., Hovestadt, D., 1996. New high temporal and spatial resolution measurements by SAMPEX of the precipitation of relativistic electrons. *Adv. Space Res.* 18 (8), 171.
- Blum, L., Li, X., Denton, M., 2015. Rapid MeV electron precipitation as observed by SAMPEX/HILT during high-speed stream-driven storms. *J. Geophys. Res.: Space Phys.* 120, 3783–3794. <http://dx.doi.org/10.1002/2014JA020633>.
- Carson, B.R., Rodger, C.J., Clilverd, M.A., 2013. POES satellite observations of EMIC-wave driven relativistic electron precipitation during 1998–2010. *J. Geophys. Res.: Space Phys.* 118, 232–243. <http://dx.doi.org/10.1029/2012JA017998>.
- Charakhch'yan, A.N., 1964. Investigation of stratosphere cosmic ray intensity fluctuations induced by processes on the Sun. *Sov. Phys. Uspekhi* 7 (3), 358–374.
- Clilverd, M.A., Seppälä, A., Rodger, C.J., Mlynczak, M.G., Kozyra, J.U., 2009. Additional stratospheric NO_x production by relativistic electron precipitation during the 2004 spring NO_x descent event. *J. Geophys. Res.* 114, A04305.
- Clilverd, M.A., Rodger, C.J., Gamble, R.J., Ulrich, T., Raita, T., Seppälä, A., Green, J.C., Thomson, N.R., Sauvaud, J.-A., Parrot, M., 2010. Ground-based estimates of outer radiation belt energetic electron precipitation fluxes into the atmosphere. *J. Geophys. Res.* 115, A12304. <http://dx.doi.org/10.1029/2010JA015638>.
- Clilverd, M.A., Duthie, R., Hardman, R., Hendry, A.T., Rodger, C.J., Raita, T., Engebretson, M., Lessard, M.R., Danskin, D., Milling, D.K., 2015. Electron precipitation from EMIC waves: a case study from 31 May 2013. *J. Geophys. Res.: Space Phys.* 120, 3618–3631. <http://dx.doi.org/10.1002/2015JA021090>.
- Comess, M.D., Smith, D.M., Selesnick, R.S., Millan, R.M., Sample, J.G., 2013. Duskside relativistic electron precipitation as measured by SAMPEX: a statistical survey. *J. Geophys. Res.: Space Phys.* 118, 5050–5058. <http://dx.doi.org/10.1002/jgra.50481>.
- Desorgher, L., Fluckiger, E.O., Moser, M.R., Butikofer, R., 2003. Geant4 simulation of the propagation of cosmic rays through the Earth's atmosphere. In: Proceedings of 28th ICRC. pp. 4277–4281.
- Desorgher, L., 2004. ATMOCOSMICS Software User Manual (<http://reat.space.qinetiq.com/septimes/atmcos>).
- Horne, R.B., 2002. The contribution of wave-particle interactions to electron loss and acceleration in the Earth's radiation belts during geomagnetic storms. In: Stone, V.R. (Ed.), *The Review of Radio Science: 1999–2002*. IEEE Press, pp. 801–828.
- Horne, R.B., Thorne, R.M., 2003. Relativistic electron acceleration and precipitation during resonant interactions with whistler-mode chorus. *Geophys. Res. Lett.* 30, L1527. <http://dx.doi.org/10.1029/2003GL016973>.
- Kalinina, O.Ya., Lazutin, L.L., Sokolov, V.D., 1988. Calculation of X-ray bremsstrahlung in the atmosphere due to the precipitation of electrons with an energy of 0.05–10 MeV. *Kosm. Luchi* 25, 107–112 (In Russian).
- Kersten, K.C., Cattell, A., Breneman, A., Goetz, K., Kellogg, P.J., Wygant, J.R., Wilson III, L.B., Blake, J.B., Looper, M.D., Roth, I., 2011. Observation of relativistic electron microbursts in conjunction with intense radiation belt whistler-mode waves. *Geophys. Res. Lett.* 38, L08107. <http://dx.doi.org/10.1029/2011GL046810>.
- Krivolutsky, A.A., Repnev, A.I., 2012. Impact of space energetic particles on the Earth's atmosphere (a review). *Geomagn. Aeron.* 52, 685–716. <http://dx.doi.org/10.1134/S0016793212060060>.
- Kubota, Y., Omura, Y., Summers, D., 2015. Relativistic electron precipitation induced by EMIC-triggered emissions in a dipole magnetosphere. *J. Geophys. Res.: Space Phys.* 120, 4384–4399. <http://dx.doi.org/10.1002/2015JA021017>.
- Lazutin, L.L., 1979. X-ray Emission of Auroral Electrons and Dynamic of the Magnetosphere. *Nauka, Moscow* (120 p. In Russian).
- Lazutin, L.L., Zhulin, I.A., Radkevich, V.A., et al., 1982. Relationship between bursting structures and pulsations of precipitating electrons, energetic particles in the Earth's magnetosphere. pp. 99–111, Apatity. (in Russian).
- Lazutin, L.L., 1986. X-ray emission of auroral electrons and magnetospheric dynamics. *Phys. Chem. Space* 14, Springer, Berlin 220.
- Li, Z., Millan, R.M., Hudson, M.K., 2013. Simulation of the energy distribution of relativistic electron precipitation caused by quasi-linear interactions with EMIC waves. *J. Geophys. Res.: Space Phys.* 118, 1–8. <http://dx.doi.org/10.1002/2013JA019163>.
- Lorentzen, K.R., McCarthy, M.P., Parks, G.K., Foat, J.E., Millan, R.M., Smith, D.M., Lin, R.P., Treilhou, J.P., 2000. Precipitation of relativistic electrons by interaction with EMIC waves. *J. Geophys. Res.* 105 (A3), 5381–5389.
- Makhmutov, V.S., Bazilevskaya, G.A., Krainev, M.B., Storini, M., 2001. Long-term cosmic ray experiment in the atmosphere: energetic electron precipitation events during the 20–23 solar activity cycles. In: Proceedings of the 27th ICRC. Hamburg, Germany, SH. pp. 4196–4199.
- Makhmutov, V.S., Storini, M., Bazilevskaya, G.A., Krainev, M.B., 2002. Observation of energetic electron precipitation events in the Southern polar atmosphere. In: M. Colacino (ed.), Proceedings of the 9th Workshop Italian Research on Antarctic Atmosphere. Roma, 2001. SIF, Bologna, vol. 80, pp. 433–443.
- Makhmutov, V.S., Bazilevskaya, G.A., Krainev, M.B., 2003a. Characteristics of the energetic electron precipitation into the Earth's polar atmosphere and geomagnetic conditions. *Adv. Space Res.* 31, 1087–1092.
- Makhmutov, V.S., Bazilevskaya, G.A., Krainev, M.B., et al., 2003b. Results of the analysis of electron precipitation events observed in the polar atmosphere. In: Physics of Auroral Phenomena, Proceedings of the XXVI Annual Seminar. Apatity, pp. 70–75.
- Makhmutov, V.S., Bazilevskaya, G.A., Stozhkov, Yu.I., Svirzhevsky, N.S., 2003c. Observations of relativistic electron precipitation events in the polar atmosphere: events characteristics and their occurrence conditions. In: Proceedings of the VII Pulkovo International Conference. GAO RAS, pp. 299–304.
- Makhmutov, V.S., Bazilevskaya, G.A., Stozhkov, Yu.I., Svirzhevskaya, A.K., Svirzhevsky, N.S., 2005. Long-term balloon cosmic ray experiment: Results of analysis of energetic electron precipitation events. *Int. J. Mod. Phys. A* 20 (29), 6843–6845.

- Makhmutov, V.S., Bazilevskaya, G.A., Desorgher, L., Flückiger, E., 2006. Precipitating electron events in October 2003 as observed in the polar atmosphere. *Adv. Space Res.* 38, 1642–1646.
- Makhmutov, V.S., Bazilevskaya, G.A., Stozhkov, Y.I., Svirzhevskaya, A.K., Svirzhevsky, N.S., 2012. Energetic electron precipitation events recorded in the Earth's polar atmosphere. In: Proceedings of the 32nd ICRC. Beijing, China, 2011. IHEP, Beijing, vol. 6, pp. 17–20.
- Meredith, N.P., Horne, R.B., Summers, D., Thorne, V., Iles, R.H.A., Heynderickx, D., Anderson, R.R., 2002. Evidence for acceleration of outer zone electrons to relativistic energies by whistler mode chorus. *Ann. Geophys.* 20, 967–979.
- Millan, R.M., Lin, R.P., Smith, D.M., Lorentzen, K.R., McCarthy, M.P., 2002. X-ray observations of MeV electron precipitation with a balloon-borne germanium spectrometer. *Geophys. Res. Lett.* 29 (24), 2194. <http://dx.doi.org/10.1029/2002GL015922>.
- Millan, R.M., Lin, R.P., Smith, D.M., McCarthy, M.P., 2007. Observation of relativistic electron precipitation during a rapid decrease of trapped relativistic electron flux. *Geophys. Res. Lett.* 34, L10101. <http://dx.doi.org/10.1029/2006GL028653>.
- Nakamura, R., Isowa, M., Kamide, Y., Baker, D.N., Blake, J.B., Looper, M., 2000. SAMPEX observations of precipitation bursts in the outer radiation belt. *J. Geophys. Res.* 105 (15), 875.
- O'Brien, T.P., Lorentzen, K.R., Mann, I.R., Meredith, N.P., Blake, J.B., Fennell, J.F., Looper, M.D., Milling, D.K., Anderson, R.R., 2003. Energization of relativistic electrons in the presence of ULF power and MeV microbursts: Evidence for dual ULF and VLF acceleration. *J. Geophys. Res.* 108 (A8), 1329. <http://dx.doi.org/10.1029/2002JA009784>.
- Parks, G.K., Freeman, T.J., McCarthy, M.P., Werden, S.H., 1993. The discovery of auroral X-rays by balloon-borne detectors and their contributions to magnetospheric research. In: Lysak, Robert L. (Ed.), *Auroral Plasma Dynamics, Geophysical Monograph 80*. American Geophysical Union, Washington, DC, p. 17.
- Picone, J.M., Hedin, A.E., Drob, D.P., Aikin, A.C., 2002. NRLMSISE-00 empirical model of the atmosphere: statistical comparisons and scientific issues. *J. Geophys. Res.* 107 (A12). <http://dx.doi.org/10.1029/2002JA009430>, SIA 15-1–SIA 15-16.
- Reeves, G.D., McAdams, K.L., Friedel, R.H.W., 2003. Acceleration and loss of relativistic electrons during geomagnetic storms. *Geophys. Res. Lett.* 30 (10), 1529. <http://dx.doi.org/10.1029/2002GL016513>.
- Sample, J.G., 2013. The MINIS balloon campaign: duskside relativistic electron precipitation. UC Berkeley: Physics. Retrieved from: (<https://escholarship.org/uc/item/7d30h592>).
- Sandanger, M.L., Søråas, F., Sørbo, M., Aarsnes, K., Oksavik, K., Evans, D.S., 2009. Relativistic electron losses related to EMIC waves during CIR and CME storms. *J. Atmos. Sol. Terr. Phys.* 71, 1126–1144.
- Spence, H.E., Reeves, G.D., Baker, D.N., Blake, J.B., Bolton, M., 2013. Science goals and overview of the Radiation Belt Storm Probes (RBSP) energetic particle, composition, and thermal plasma (ECT) suite on NASA's Van Allen Probes Mission. *Space Sci. Rev.* 179, 311–336. <http://dx.doi.org/10.1007/s11214-013-0007-5>.
- Stozhkov, Y.I., Svirzhevsky, N.S., Makhmutov, V.S., 2001. Cosmic ray measurements in the atmosphere. In: Kirkby, J. (ed.), *Workshop on Ion-Aerosol-Cloud Interactions*, CERN, CERN-2001-007, Experimental Phys. Division, Geneva, CERN Scientific Information Service, vol. 640, pp. 41–62.
- Stozhkov, Y.I., Svirzhevsky, N.S., Bazilevskaya, G.A., Kvashnin, A.N., Makhmutov, V.S., Svirzhevskaya, A.K., 2009. Long-term (50 years) measurements of cosmic ray fluxes in the atmosphere. *Adv. Space Res.* 44 (10), 1124–1137.
- Turunen, E., Verronen, P.T., Seppälä, A., Craig, J., Rodger, J., Mark, A., Clilverd, M.A., Tamminen, J., Enell, C.-F., Ulich, T., 2009. Impact of different energies of precipitating particles on NO_x generation in the middle and upper atmosphere during geomagnetic storms. *J. Atmos. Sol. Terr. Phys.* 71, 1176–1189.
- Ukhorskiy, Y., Sitnov, M.I., Millan, R.M., Kress, B.T., Fennell, J.F., Claudepierre, S.G., Barnes, R.J., 2015. Global storm time depletion of the outer electron belt. *J. Geophys. Res.: Space Phys.* 120, 2543–2556. <http://dx.doi.org/10.1002/2014JA020645>.
- Wang, Z., Yuan, Z., Li, M., Li, H., Wang, D., Li, H., Huang, S., Qiao, Z., 2014. Statistical characteristics of EMIC wave-driven relativistic electron precipitation with observations of POES satellites: Revisit. *J. Geophys. Res.: Space Phys.* 119, 5509–5519. <http://dx.doi.org/10.1002/2014JA020082>.
- Woodger, L.A., Halford, A.J., Millan, R.M., McCarthy, M.P., Smith, D.M., Bowers, G.S., Sample, J.G., Anderson, B.R., Liang, X., 2015. A summary of the BARREL campaigns: technique for studying electron precipitation. *J. Geophys. Res.: Space Phys.* 120, 4922–4935. <http://dx.doi.org/10.1002/2014JA020874>.